Cell Reports
Report

Conservation of a Triple-Helix-Forming RNA Stability Element in Noncoding and Genomic RNAs of Diverse Viruses

Kazimierz T. Tycowski,[1] Mei-Di Shu,[1] Sumit Borah,[1] Mary Shi,[1] and Joan A. Steitz[1,*]
[1]Department of Molecular Biophysics and Biochemistry, Howard Hughes Medical Institute, Yale University School of Medicine, 295 Congress Avenue, New Haven, CT 06536, USA
*Correspondence: joan.steitz@yale.edu
http://dx.doi.org/10.1016/j.celrep.2012.05.020

SUMMARY

Abundant expression of the long noncoding (lnc) PAN (polyadenylated nuclear) RNA by the human oncogenic gammaherpesvirus Kaposi's sarcoma-associated herpesvirus (KSHV) depends on a *cis*-element called the expression and nuclear retention element (ENE). The ENE upregulates PAN RNA by inhibiting its rapid nuclear decay through triple-helix formation with the poly(A) tail. Using structure-based bioinformatics, we identified six ENE-like elements in evolutionarily diverse viral genomes. Five are in double-stranded DNA viruses, including mammalian herpesviruses, insect polydnaviruses, and a protist mimivirus. One is in an insect picorna-like positive-strand RNA virus, suggesting that the ENE can counteract cytoplasmic as well as nuclear RNA decay pathways. Functionality of four of the ENEs was demonstrated by increased accumulation of an intronless polyadenylated reporter transcript in human cells. Identification of these ENEs enabled the discovery of PAN RNA homologs in two additional gammaherpesviruses, RRV and EHV2. Our findings demonstrate that searching for structural elements can lead to rapid identification of lncRNAs.

INTRODUCTION

Both cellular and viral mRNAs are subject to robust RNA decay pathways. Most mRNAs undergo cytoplasmic decay initiated by poly(A) tail shortening followed by decapping and degradation of the transcript body (Chen and Shyu, 2011; Garneau et al., 2007). Parallel decay pathways in the nucleus act in quality control systems that degrade aberrant transcripts (Doma and Parker, 2007; Schmid and Jensen, 2010), but also influence the levels of normal mRNAs (Kuai et al., 2005). Because of structural similarity to mRNA, long noncoding (lnc) RNAs may be subject to the same RNA decay mechanisms (Conrad et al., 2006; Geisler et al., 2012; Thompson and Parker, 2007). Since these decay pathways often initiate with deadenylation, abundant polyadenylated RNAs frequently harbor *cis*-acting elements that protect their poly(A) tails (Conrad et al., 2006; Conrad and Steitz, 2005; Garneau et al., 2008; Muhlrad and Parker, 2005; Wang et al., 1999).

Polyadenylated nuclear (PAN) RNA (also known as T1.1 or nut-1 RNA) is a lncRNA produced by the oncogenic gammaherpesvirus, Kaposi's sarcoma-associated herpesvirus (KSHV) (Sun et al., 1996; Zhong and Ganem, 1997). PAN RNA accumulates to extraordinarily high levels (~500,000 copies/cell) during lytic infection and is required for the production of late viral proteins and infectious virus (Borah et al., 2011; Sun et al., 1996). The expression and nuclear retention element (ENE), located ~120 nt upstream of PAN RNA's polyadenylation site, is essential for this high accumulation (Conrad et al., 2006; Conrad and Steitz, 2005). The ENE inhibits rapid decay of PAN RNA by blocking deadenylation (Conrad et al., 2006, 2007). It also stabilizes heterologous intronless transcripts, but does not affect the translation of reporter mRNAs (Conrad and Steitz, 2005; Pawlicki and Steitz, 2008).

The KSHV ENE is a 79 nt long RNA element, composed of a stem-loop structure with an asymmetric internal U-rich loop, which in conjunction with adjacent base pairs constitutes the ENE's functional core (Conrad et al., 2007) (Figure 1A). The crystal structure of the ENE core bound to oligo(A)$_9$ revealed 5 consecutive U-A:U base triples formed between the U-rich loop and oligo(A)$_9$ (Mitton-Fry et al., 2010); binding is extended by A-minor interactions with three G-C base pairs of the lower stem. Genetic and biochemical analyses indicate similar interactions between the PAN RNA's poly(A) tail and the ENE in vivo (Conrad et al., 2007; Mitton-Fry et al., 2010).

Because lncRNAs are poorly conserved (Pang et al., 2006; Ulitsky et al., 2011), sequence homology searches often fail to identify homologs even from closely related organisms. However, they can possess conserved structural elements (Parker et al., 2011; Stadler, 2010), suggesting that structure-based queries may be more powerful. Numerous bioinformatics tools for RNA structure analysis were developed and used to identify small noncoding RNAs (Cruz and Westhof, 2011; Eddy, 2006; Menzel et al., 2009; Washietl, 2010).

Here, by devising a structure-based bioinformatics approach, we identified six ENE-like elements in diverse viral genomes; five in double-stranded DNA (dsDNA) viruses (herpesviruses, bracoviruses [Dupuy et al., 2006], and mimiviruses [Claverie et al., 2009]) and one in a positive-strand RNA virus (picorna-like dicistrovirus [Bonning and Miller, 2010]). We tested four structures

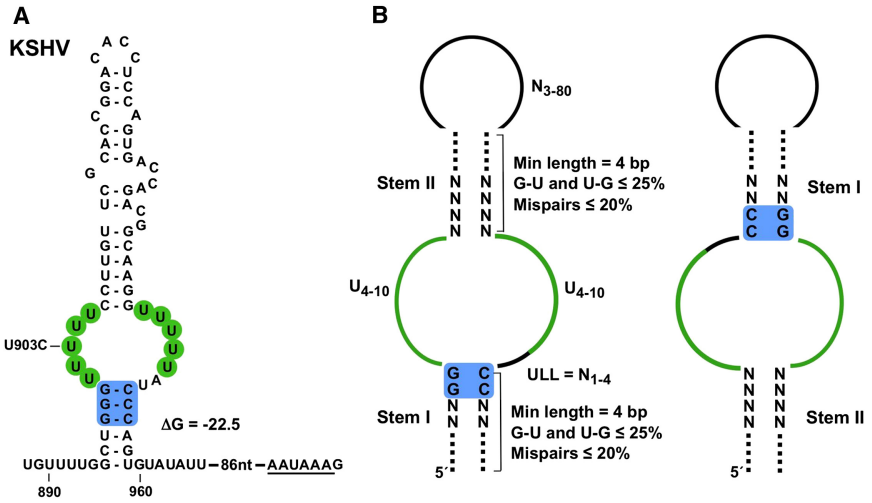

Figure 1. ENE Models for Designing the RNAMotif Descriptors

(A) Secondary structure of the KSHV PAN ENE with unfolded flanking sequences. Free energy (ΔG in kcal/mol) is for the folded ENE only. The U residues involved in triple-helix formation with poly(A) and the G-C base pairs involved in A-minor interactions are shaded green and blue, respectively. The polyadenylation signal is underlined. Nucleotide numbering is relative to the 5′ end of PAN RNA. The U903C mutant (Conrad et al., 2007) was used for Figure 4D.

(B) Models of the ENE in standard (left) and inverted (right) configuration. Parameters for the RNAMotif search are shown (see Experimental Procedures for details), where N = A, C, G or U and ULL = the U-rich loop linker.

and demonstrated their functionality in increasing the accumulation of a reporter RNA. The ENEs in the dsDNA viruses all map to intergenic regions, suggesting the existence of unidentified lncRNAs. Indeed, we confirmed the ENE-dependent expression of one of these lncRNAs, which appears to be a homolog of the KSHV PAN RNA, in rhesus rhadinovirus (RRV).

RESULTS

To search for novel ENEs, we designed a bioinformatic screen utilizing the RNAMotif (Macke et al., 2001), Mfold (Zuker, 2003), and BLAST algorithms. Previous mutational (Conrad et al., 2007) and crystallographic (Mitton-Fry et al., 2010) analyses defined functionally important residues and secondary structure features of the KSHV ENE (see Figure 1A). We incorporated these into ENE models (Figure 1B) that served as a basis for designing RNAMotif descriptors allowing (1) the U-rich internal loop to have 4–10 U residues on each side for formation of a triple helix with poly(A), and (2) the flanking stems to be at least 4 bp long, with stem I capped by two G-C base pairs to facilitate A-minor interactions (see Experimental Procedures for details). The size of the internal loop and length of the stems were chosen arbitrarily. We reasoned that an ENE could assume two orientations within an RNA: standard (left panel) or inverted (right panel).

Identification of ENEs

We searched available viral sequences, considering only eukaryotic viruses because of the interaction with the poly(A) tail by the original KSHV ENE. Our search yielded fourteen hits in nine different viruses. Of these, we consider 12 from 7 viruses to represent ENEs because (1) they exhibit common features not included in our bioinformatics selection, and (2) the appearance of either a polyadenylation signal (AAUAAA or AUUAAA) or a genomically encoded poly(A) tract within 200 nucleotides downstream. Of the 12 ENE hits, 7 are unique, including the KSHV ENE (Figures 1A and 2A). Two are from other gammaherpesviruses, RRV and equine herpesvirus 2 (EHV2 [Telford et al., 1995]) (see Figure S1A for phylogenetic distribution) and seven appear in two polydnaviruses, *Cotesia congregata* and *Cotesia sesamiae* bracoviruses (Dupuy et al., 2006). While each gammaherpesvirus possesses a single ENE, the *C. congregata* bracovirus contains six (four identical and two variant copies that differ by one or two residues) in different genomic regions (data not shown). We found only one ENE in *C. sesamiae* bracovirus, but the genome is only partially sequenced. One ENE structure appears in *Acanthamoeba polyphaga* mimivirus (Claverie et al., 2009). Interestingly, our screen identified an ENE candidate in a positive-strand picorna-like virus, *Plautia stali* intestine virus (PSIV) (Sasaki et al., 1998).

The ENEs of RRV, EHV2, *C. congregata* and *C. sesamiae* bracoviruses and *A. polyphaga* mimivirus all lie within predicted intergenic regions (Figure 2B and data not shown). In PSIV, the ENE is located in the region of the genomic RNA corresponding to the 3′ untranslated region (UTR) when the genome serves as a mRNA (Figure S1B); a poly(A) stretch is genetically encoded 106 nt downstream of the ENE.

Each ENE (Figure 2A) can assume an imperfect stem-loop structure with a U-rich internal loop predicted to form 4, 5, or 6 U-A:U base triples with an oligo(A) sequence. They also possess several common features not inferred previously from functional analyses of the KSHV ENE, including (1) a conserved U-A base pair (A-U in the inverted ENEs) in stem I, and (2) a biased nucleotide distribution in stem II, which is pyrimidine-rich near the U-rich loop on the 5′ side (3′ side in the inverted ENEs) paired to a purine-rich complementary strand.

Functionality of the Newly Discovered ENEs

To address whether the newly discovered ENEs function in RNA stabilization, we tested four structures for their ability to increase accumulation of an intronless β-globin mRNA reporter (Conrad and Steitz, 2005). One or two copies of the RRV, EHV2, *C. congregata* bracovirus or PSIV ENE were inserted 167 nt upstream of the polyadenylation site in the 179 nt long β-globin 3′ UTR and the resulting chimeras transiently expressed in HEK293T cells. Figure 3 shows that, relative to the no insert control (lane 1), one copy of the KSHV ENE increased β-globin mRNA levels 9.2-fold (lane 2), whereas the RRV and EHV2 ENEs showed 3.2- and 2-fold stabilization, respectively (lanes

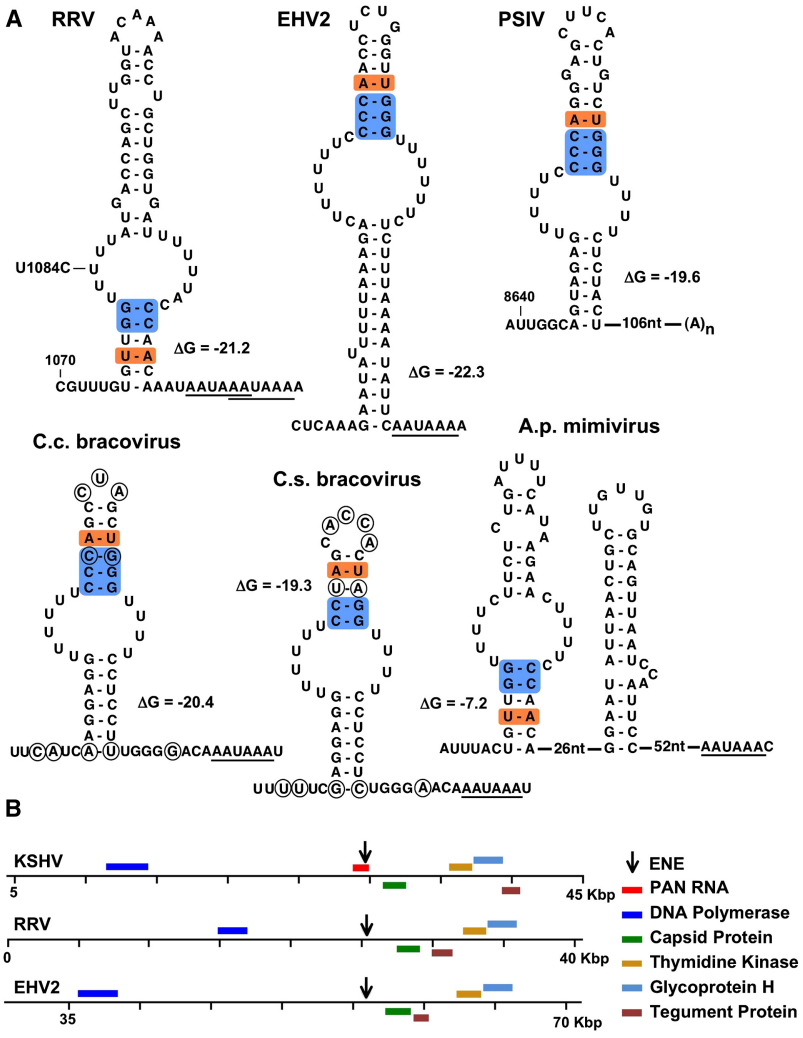

Figure 2. Newly Discovered ENEs

(A) Secondary structures were predicted using the Mfold program with unfolded 5′ and 3′ flanking sequences. Free energies (ΔG in kcal/mol) were calculated for the folded ENE structures only. Base pairs predicted to be involved in A-minor interactions with poly(A) targets are shaded blue. A conserved U-A (A-U in inverted ENEs) base pair is shaded orange. Polyadenylation signals are underlined. In the *A. polyphaga* (A.p.) mimivirus, the 3′ proximal stem loop may direct alternative polyadenylation within the stem loop itself, as documented for mimivirus transcripts (Byrne et al., 2009). In RRV and PSIV, the nucleotide numbering is relative to the 5′ end of PAN RNA and genomic RNA, respectively. The U1084C mutation in the RRV ENE used in Figure 4D is indicated. Circled nucleotides in bracoviruses are different in *C. congregata* (C.c.) and *C. sesamiae* (C.s.).

(B) Location of ENEs in gammaherpesvirus genomes; only ORFs that are conserved in all gammaherpesviruses and KSHV PAN RNA are shown.

See also Figure S1.

4 and 6). The single *C. congregata* bracovirus and PSIV ENEs showed 1.7- and 1.1-fold increase, respectively (lanes 14 and 16). Two copies of each ENE exhibited about 3-fold stronger stabilization activity than one. None of the ENE inserts in antisense orientation increased the levels of β-globin mRNA, but slightly lowered its accumulation (compare lanes 8–12 with 1 and 18–21 with 13). In summary, all of the ENEs tested increased accumulation of the intronless β-globin transcript, but to varying degrees.

RRV Expresses an ENE-Containing PAN RNA Homolog

Within the gammaherpesvirus genomes, the ENEs map to syntenic regions (Figure 2B), arguing that they are transcribed within as yet unidentified PAN RNA homologs. Thus, we asked whether an ENE-containing RNA is made in the RRV lytic phase. Latently infected BJAB-RRV-GFP cells were treated with trichostatin A (TSA) to reactivate the virus (DeWire and Damania, 2005), and total cellular RNA collected one or two days later was analyzed by northern blotting (Figure 4A). An oligonucleotide probe complementary to the RRV ENE sequence revealed a 1.3 kb transcript in RRV-infected (lanes 3–6) but not uninfected (lane 2) BJAB cells. Transcript levels increased dramatically one day after lytic reactivation of the virus (compare lane 3 with 4 and 5 with 6). The 1.3 kb RNA was retained on oligo(dT) cellulose as efficiently as GAPDH mRNA (lanes 7 and 8), consistent with two overlapping AAUAAA polyadenylation signals 3 and 7 nt downstream of the ENE (see Figure 2A). 3′ RACE analysis mapped a poly(A) tail beginning 27 nt 3′ to the ENE (data not shown). Primer extension analysis (Figure S2) mapped the 5′ end 1157 nt upstream of the polyadenylation site.

The 1.3 kb RRV polyadenylated RNA exhibits little sequence similarity to KSHV PAN RNA and appears to be likewise noncoding (Figure S3). The longest open reading frame (ORF) encodes only 34 amino acids and is preceded by multiple AUG codons (data not shown). The 1.3 kb sequence is strikingly repetitive; in its 3′ portion, about 40 nt upstream of the ENE, 26 nt are repeated ten times to form a perfect array (schematized in Figure 4B). In its 5′ portion, shorter more dispersed AU-rich repeats appear.

We tested the 1.3 kb RRV RNA for three hallmarks of the KSHV PAN RNA: nuclear localization (Sun et al., 1996), dependence on viral ORF50/Rta for expression (Chang et al., 2002) and upregulation by the viral SOX protein (Borah et al., 2011). BJAB-RRV-GFP cells, which spontaneously reactivate the virus at low frequency and give a strong GFP signal, react with the probe for the 1.3 kb RNA and show relocalization of the normally cytoplasmic poly(A)-binding protein C1 (PABPC1) to the nucleus (Figure 4C). The 1.3 kb RNA and nuclear PABPC1 signals largely coincide, as previously observed for KSHV PAN RNA (Borah et al., 2011). To test for dependence on ORF50/Rta and for upregulation by SOX, we transiently expressed the 1.3 kb RNA in HEK293T cells in the absence or presence of either RRV ORF50/Rta or both ORF50/Rta and the KSHV SOX protein (Figure S4). As for KSHV PAN RNA, expression is completely

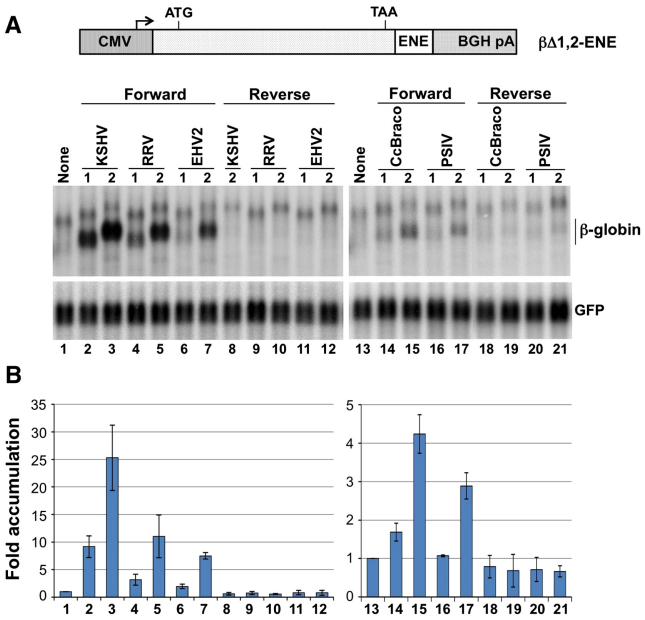

Figure 3. ENEs Increase the Levels of a Heterologous Intronless Transcript

β-globin constructs (βΔ1,2-ENE) containing either one or two copies of the KSHV, RRV, EHV2, *C. congregata* bracovirus (CcBraco) or PSIV ENE were transiently expressed in HEK293T cells. ENE inserts were in either forward or reverse orientation.

(A) Northern blot analysis of β-globin mRNA using a full-size RNA probe. The same blot was probed with the SB180 oligonucleotide for GFP mRNA expressed from a cotransfected plasmid. The band above β-globin mRNA may represent a nonpolyadenylated precursor.

(B) Quantification of northern blot signals. To control for transfection efficiency and loading, the levels of β-globin transcripts were normalized to those of GFP mRNA. The βΔ1,2 signal (lanes 1 and 13) was set to 1. Bars depict the average values from three experiments; error bars show SD.

dependent on ORF50/Rta (compare lane 2 to 1) and is upregulated 3-fold by the SOX protein (lane 3). We conclude that the RRV 1.3 kb RNA exhibits features of KSHV PAN RNA and is likely to be a homolog.

RRV ENE Is Required for Accumulation of RRV PAN RNA

Since the effect of the RRV ENE on β-globin mRNA accumulation is about 3-fold less than that of its KSHV counterpart (Figure 3), we assessed its importance for the accumulation of its host RNA, RRV PAN. We expressed WT PAN RNA, the ENE deletion, and ENE point mutants (indicated in Figures 1A and 2A) from both viruses in HEK293T cells (Figure 4D), along with control GFP mRNA. Deletion of the entire ENE (lane 2) or substitution of a single U residue by C in the U-rich loop (U1084C mutant, lane 3) resulted in a 4-fold reduction in RRV PAN expression, comparable to that observed for the KSHV PAN RNA with analogous changes (lanes 5 and 6). Thus, an ENE is as important for cellular accumulation of RRV PAN RNA as it is for its KSHV counterpart.

A Putative PAN RNA Homolog in EHV2

Despite little overall sequence conservation of KSHV and RRV PAN RNAs (Figure S3 and data not shown), their first 25 nt exhibit similarity that extends into the PAN RNA promoters. Using these conserved sequences as a query, we searched the EHV2 genome and identified promoter and transcription start site signals for the EHV2 PAN RNA 1,708 nt upstream of the ENE. On the 3′ side, the EHV2 ENE abuts an AAUAAA polyadenylation signal (see Figure 2A). Because of downstream homology to KSHV and RRV, we predict a polyadenylation site 19 nt 3′ to the EHV2 ENE. Thus, the putative EHV2 PAN RNA is 1,789 nt long, with the longest ORF (20 amino acids) preceded by multiple AUG codons and not significantly conserved in RRV or KSHV (data not shown).

DISCUSSION

Despite identification of numerous abundant lncRNAs from both cellular (Hogan et al., 1994; Hutchinson et al., 2007; Jolly et al., 2004; Pontier and Gribnau, 2011) and viral (Bermudez-Cruz et al., 1997; Sun et al., 1996) sources, little is known about mechanisms underlying their cellular accumulation. For KSHV PAN lncRNA, not only high levels of transcription, but also increased stability via two RNA elements, the ORE and the ENE, contribute (Conrad et al., 2006; Conrad and Steitz, 2005; Sahin et al., 2010). For 7 years, KSHV PAN RNA has been the only lncRNA known to possess an ENE (Conrad and Steitz, 2005). Here, we identified six ENEs in diverse viral genomes, including one ssRNA and five dsDNA viruses (Figure 2A). Four tested ENEs all increased the levels of an intronless β-globin transcript, demonstrating stabilization activity (Figure 3). We also showed that the RRV ENE is required for high accumulation of a novel RRV transcript (Figure 4), the first homolog of KSHV PAN RNA to be identified.

The other five ENEs are elements that likely contribute to the stability of their host RNAs since they share with KSHV and RRV features not selected in our bioinformatics screen (Figures 1A and 2A). First, they are located either near polyadenylation signals (EHV2, bracoviruses, and mimivirus) or near a genetically encoded poly(A) stretch (PSIV). Second, they possess common characteristics of unknown function within the stems of the ENE itself: (1) a conserved U-A base pair (A-U in the inverted ENEs) in stem I, and (2) a biased nucleotide distribution in stem II, which is pyrimidine-rich close to the U-rich loop at the 5′ side (3′ side in the inverted ENEs). A third feature, suggesting functional conservation of bracovirus ENEs, is compensatory mutations that ensure stem integrity (Figure 2A).

Although some ENEs increase the levels of the β-globin reporter only marginally (Figure 3), they may be more potent in their natural contexts. Specifically, the RRV ENE is 3 times less stabilizing in a heterologous β-globin mRNA than the KSHV ENE (Figure 3), but comparably upregulates its host transcript (4-fold) relative to the ΔENE construct (Figure 4D). Perhaps the short distance between the ENE and the poly(A) tail (26 nt compared to 117 nt for RRV versus KSHV) is critical for efficient upregulation, although the influence of surrounding sequences cannot be excluded. At least in herpesviruses, the weaker the ENE in reporter upregulation, the closer to the polyadenylation signal it resides (see Figures 1A, 2A, and 3). The importance of distance from the poly(A) tail requires further investigation.

Discovery of an ENE in PSIV argues for a cytoplasmic function, presumably in RNA stabilization, contrary to previous

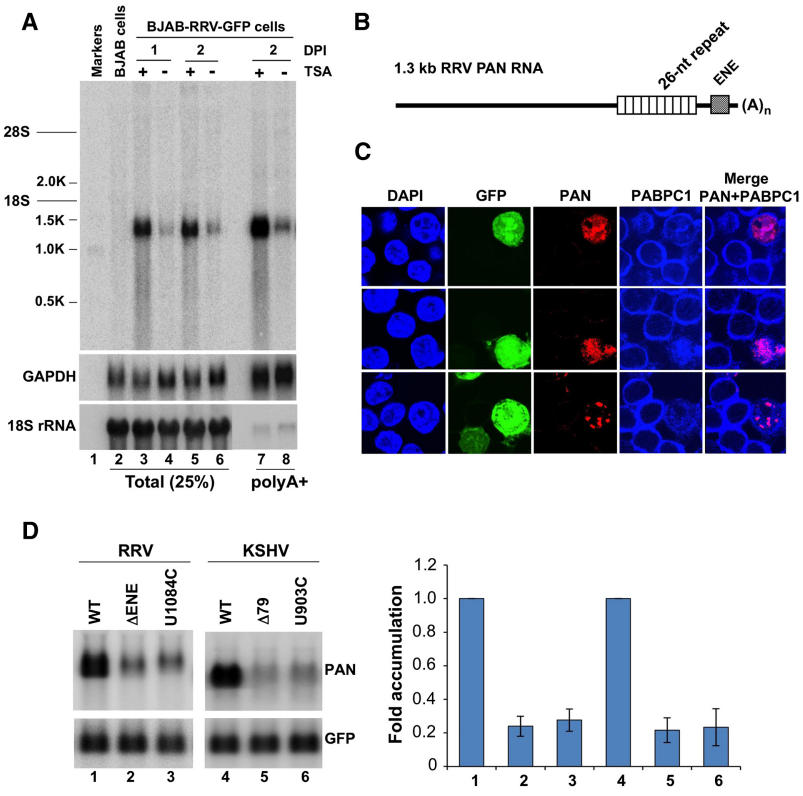

Figure 4. RRV Expresses an ENE-Containing Polyadenylated RNA

(A) To probe for an ENE-containing transcript(s), total cellular (lanes 3-6) or poly(A)$^+$ (lanes 7 and 8) RNA from BJAB-RRV-GFP cells, either untreated or treated with TSA as indicated, was analyzed by northern blot hybridization using oligonucleotide KT492, complementary to a portion of the RRV ENE. Lane 2 shows total RNA from uninfected BJAB cells. The same blot was reprobed for GAPDH mRNA and 18S rRNA using a mixture of the SB71 and SB87 probes, and the SB231 probe, respectively. DPI, days postinduction.

(B) Schematic of 1.3 kb RRV PAN RNA; not drawn to scale.

(C) Subcellular localization of 1.3 kb RRV PAN RNA (red) and nuclear PABPC1 (blue) in BJAB-RRV-GFP cells with the reactivated virus (green). Three different fields are shown.

(D) The ENE is required for high accumulation of the RRV PAN RNA. The ΔENE and Δ79 (Conrad and Steitz, 2005) deletion mutations encompass the entire ENE structures in RRV and KSHV PAN RNAs, respectively. Positions of the U903C and U1084C point mutations are indicated in Figures 1A and 2A, respectively. The WT or mutant PAN RNA gene derived from either RRV or KSHV was transiently expressed in HEK293T cells as indicated. The KSHV and RRV PAN RNAs were detected by northern blotting using the SB2 and KT493 probes, respectively. The same blot was reprobed with the SB180 oligonucleotide for GFP mRNA expressed from a cotransfected plasmid. The bar graph shows average values from three experiments; error bars represent SD. Levels of β-globin transcripts were normalized to those of GFP mRNA; levels of the WT RNAs were set to 1.

See also Figures S2, S3, and S4.

conclusions about ENE effectiveness in the cytoplasm (Conrad and Steitz, 2005). The genomic RNAs of positive-strand RNA viruses commonly harbor other stabilization elements (Garneau et al., 2008; Sharma et al., 2009), and the ENE may add to this list. Alternatively, the putative interaction between the ENE and the poly(A) tail could serve a distinct role, such as contributing to a network of RNA/RNA interactions found in the 3′ UTRs of positive-strand RNA viruses (Liu et al., 2009). In related picornaviruses (e.g., poliovirus) such assemblies involve the poly(A) tail and are essential for genome replication (Liu et al., 2009; Zoll et al., 2009).

Structural characterization of the KSHV ENE (Mitton-Fry et al., 2010) enabled identification of a PAN RNA homolog in RRV and a putative homolog in EHV2. A long, apparently noncoding, polyadenylated transcript, L1.7 RNA, is abundantly expressed from the syntenic region of yet another gammaherpesvirus, bovine herpesvirus 4 (BHV4) (Bermudez-Cruz et al., 1997). Although the KSHV and RRV PAN RNAs, as well as their putative EHV2 homolog, exhibit little sequence similarity to L1.7 RNA, their promoters and the sequences surrounding their transcription start and polyadenylation sites are significantly conserved (Figure S3). Another common feature is the presence of repetitive sequences. Thus, L1.7 RNA may be a BHV4 PAN RNA homolog, although neither our bioinformatic screen nor careful inspection revealed an ENE-like structure. If some gammaherpesviruses produce ENE-less PAN RNA homologs, then our observations argue that PAN RNAs are widely expressed among gammaherpesviruses. The identification of homologs in RRV and EHV2 will aid in elucidating why PAN RNA is essential for the expression of late viral proteins (Borah et al., 2011; Rossetto and Pari, 2012). Genetic manipulation of the KSHV PAN RNA locus has been difficult because of the overlap with an important protein-coding gene, *K7* (Wang et al., 2002). Since PAN RNA genes in RRV and EHV2 do not overlap predicted ORFs, this problem can be circumvented allowing mechanistic studies.

Although ENEs are relatively rare, their occurrence in evolutionarily divergent viruses raises the question of their presence in cellular RNAs. Six additional ENE structures will facilitate derivation of more defined consensus features for searching larger sequence datasets, e.g., vertebrate genomes. Importantly, this work demonstrates that structural elements can be effectively used for the rapid identification of homologous and possibly unrelated lncRNAs, even in the absence of sequence conservation.

EXPERIMENTAL PROCEDURES

Bioinformatics

The viral genomic RefSeq database (NCBI, release 43) was queried for ENEs using RNAMotif (Macke et al., 2001). We reasoned that if the ENE's functional core is embedded within a larger nonconserved sequence, it might be more easily detected with a descriptor-based algorithm rather than probabilistic model-based tools like RSEARCH or Infernal (Eddy, 2006). The ENE descriptors were based on the models shown in Figure 1B, with lengths of the stems and loops chosen arbitrarily. Each descriptor required that (1) both stems be at

least 4 bp long with stem I capped by two G-C base pairs, (2) the U-rich internal loop contain symmetrical numbers (4–10) of Us on each side, and (3) the U-rich loop linker be 1 to 4 nt long. The sequence closing the upper stem varied between 3 and 80 nt. Each stem was permitted to possess a maximum of 25% wobble base pairs and 20% mispairs. Only hits with $\Delta G \leq -5$ kcal/mol were accepted. Because of the high background of false-positive hits, additional selection was required. Thus, the RNAMotif hits were folded with Mfold (Zuker, 2003) and only those that could assume ENE-like structures with $\Delta G \leq$ the ΔG of alternative folds were accepted. Successful hits were used to query viral sequences in the NCBI nonredundant database using BLAST.

The currently available genomes of 50 herpesviruses (NCBI) were similarly scanned for ENEs with one or more single-nucleotide bulge(s) in their stems. No additional ENEs were identified.

Cell Culture, Transfections, and RNA Analyses

HEK293T cells were grown in DMEM medium with 10% fetal bovine serum (FBS) and transfections were performed using TransIT-293 (Mirus) according to the manufacturer's protocol. BJAB and BJAB-RRV-GFP (DeWire and Damania, 2005) cells were cultured in RPMI 1640 medium with 10% FBS. For viral reactivation, BJAB-RRV-GFP cells were grown in the presence of 100 nM TSA (Sigma). For northern blot analyses and 5′ end mapping, RNA was isolated using Trizol (Life Technologies). To detect β-globin RNAs, a uniformly ^{32}P-labeled full-length RNA probe was used. Other RNAs were detected with 5′-^{32}P-labeled DNA oligonucleotides.

Immunofluorescence and In Situ Hybridization

BJAB-RRV-GFP cells (DeWire and Damania, 2005) were immobilized on glass slides coated with poly-L-lysine (Sigma-Aldrich), and IF and FISH were performed as described (Pawlicki and Steitz, 2008). RRV PAN RNA was detected with a mixture of KT492 and KT493 probes (Supplemental Information) labeled with digoxigenin-dUTP and visualized with rhodamine-conjugated anti-digoxigenin antibody (Jackson Lab Immunologicals). PABPC1 was detected with rabbit polyclonal antibody (Abcam) and Alexafluor 660-conjugated anti-rabbit secondary antibody (Invitrogen). Images were collected on a Leica TCS SP5 confocal microscope.

SUPPLEMENTAL INFORMATION

Supplemental Information includes Extended Experimental Procedures and four figures and can be found with this article online at http://dx.doi.org/10.1016/j.celrep.2012.05.020.

LICENSING INFORMATION

ACKNOWLEDGMENTS

We thank B. Damania, B. Glaunsinger, D. Kedes, and G. Miller for reagents; J. Franklin and R. Mitton-Fry for bioinformatics advice; and E. Ullu and C. Tschudi for access to their computer server. We also thank J. Brown, D. Cazalla, E. Guo, K. Riley, A. Vilborg, and A. Miccinello for critical reading of the manuscript and the entire Steitz lab for stimulating discussions. This work was supported by grants GM026154 and CA16038 from the NIH. J.A.S. is an investigator of the Howard Hughes Medical Institute.

Received: March 27, 2012
Revised: April 19, 2012
Accepted: May 23, 2012
Published online: July 5, 2012

REFERENCES

Bermudez-Cruz, R., Zhang, L., and van Santen, V.L. (1997). Characterization of an abundant, unique 1.7-kilobase bovine herpesvirus 4 (BHV-4) late RNA and mapping of a BHV-4 IE2 transactivator-binding site in its promoter-regulatory region. J. Virol. *71*, 527–538.

Bonning, B.C., and Miller, W.A. (2010). Dicistroviruses. Annu. Rev. Entomol. *55*, 129–150.

Borah, S., Darricarrère, N., Darnell, A., Myoung, J., and Steitz, J.A. (2011). A viral nuclear noncoding RNA binds re-localized poly(A) binding protein and is required for late KSHV gene expression. PLoS Pathog. *7*, e1002300.

Byrne, D., Grzela, R., Lartigue, A., Audic, S., Chenivesse, S., Encinas, S., Claverie, J.M., and Abergel, C. (2009). The polyadenylation site of Mimivirus transcripts obeys a stringent 'hairpin rule'. Genome Res. *19*, 1233–1242.

Chang, P.J., Shedd, D., Gradoville, L., Cho, M.S., Chen, L.W., Chang, J., and Miller, G. (2002). Open reading frame 50 protein of Kaposi's sarcoma-associated herpesvirus directly activates the viral PAN and K12 genes by binding to related response elements. J. Virol. *76*, 3168–3178.

Chen, C.Y., and Shyu, A.B. (2011). Mechanisms of deadenylation-dependent decay. Wiley Interdiscip Rev RNA *2*, 167–183.

Claverie, J.M., Abergel, C., and Ogata, H. (2009). Mimivirus. Curr. Top. Microbiol. Immunol. *328*, 89–121.

Conrad, N.K., and Steitz, J.A. (2005). A Kaposi's sarcoma virus RNA element that increases the nuclear abundance of intronless transcripts. EMBO J. *24*, 1831–1841.

Conrad, N.K., Mili, S., Marshall, E.L., Shu, M.D., and Steitz, J.A. (2006). Identification of a rapid mammalian deadenylation-dependent decay pathway and its inhibition by a viral RNA element. Mol. Cell *24*, 943–953.

Conrad, N.K., Shu, M.D., Uyhazi, K.E., and Steitz, J.A. (2007). Mutational analysis of a viral RNA element that counteracts rapid RNA decay by interaction with the polyadenylate tail. Proc. Natl. Acad. Sci. USA *104*, 10412–10417.

Cruz, J.A., and Westhof, E. (2011). Sequence-based identification of 3D structural modules in RNA with RMDetect. Nat. Methods *8*, 513–521.

DeWire, S.M., and Damania, B. (2005). The latency-associated nuclear antigen of rhesus monkey rhadinovirus inhibits viral replication through repression of Orf50/Rta transcriptional activation. J. Virol. *79*, 3127–3138.

Doma, M.K., and Parker, R. (2007). RNA quality control in eukaryotes. Cell *131*, 660–668.

Dupuy, C., Huguet, E., and Drezen, J.M. (2006). Unfolding the evolutionary story of polydnaviruses. Virus Res. *117*, 81–89.

Eddy, S.R. (2006). Computational analysis of RNAs. Cold Spring Harb. Symp. Quant. Biol. *71*, 117–128.

Garneau, N.L., Wilusz, J., and Wilusz, C.J. (2007). The highways and byways of mRNA decay. Nat. Rev. Mol. Cell Biol. *8*, 113–126.

Garneau, N.L., Sokoloski, K.J., Opyrchal, M., Neff, C.P., Wilusz, C.J., and Wilusz, J. (2008). The 3′ untranslated region of sindbis virus represses deadenylation of viral transcripts in mosquito and Mammalian cells. J. Virol. *82*, 880–892.

Geisler, S., Lojek, L., Khalil, A.M., Baker, K.E., and Coller, J. (2012). Decapping of long noncoding RNAs regulates inducible genes. Mol. Cell *45*, 279–291.

Hogan, N.C., Traverse, K.L., Sullivan, D.E., and Pardue, M.L. (1994). The nucleus-limited Hsr-omega-n transcript is a polyadenylated RNA with a regulated intranuclear turnover. J. Cell Biol. *125*, 21–30.

Hutchinson, J.N., Ensminger, A.W., Clemson, C.M., Lynch, C.R., Lawrence, J.B., and Chess, A. (2007). A screen for nuclear transcripts identifies two linked noncoding RNAs associated with SC35 splicing domains. BMC Genomics *8*, 39.

Jolly, C., Metz, A., Govin, J., Vigneron, M., Turner, B.M., Khochbin, S., and Vourc'h, C. (2004). Stress-induced transcription of satellite III repeats. J. Cell Biol. *164*, 25–33.

Kuai, L., Das, B., and Sherman, F. (2005). A nuclear degradation pathway controls the abundance of normal mRNAs in Saccharomyces cerevisiae. Proc. Natl. Acad. Sci. USA *102*, 13962–13967.

Liu, Y., Wimmer, E., and Paul, A.V. (2009). Cis-acting RNA elements in human and animal plus-strand RNA viruses. Biochim. Biophys. Acta *1789*, 495–517.

Macke, T.J., Ecker, D.J., Gutell, R.R., Gautheret, D., Case, D.A., and Sampath, R. (2001). RNAMotif, an RNA secondary structure definition and search algorithm. Nucleic Acids Res. *29*, 4724–4735.

Menzel, P., Gorodkin, J., and Stadler, P.F. (2009). The tedious task of finding homologous noncoding RNA genes. RNA *15*, 2075–2082.

Mitton-Fry, R.M., DeGregorio, S.J., Wang, J., Steitz, T.A., and Steitz, J.A. (2010). Poly(A) tail recognition by a viral RNA element through assembly of a triple helix. Science *330*, 1244–1247.

Muhlrad, D., and Parker, R. (2005). The yeast EDC1 mRNA undergoes deadenylation-independent decapping stimulated by Not2p, Not4p, and Not5p. EMBO J. *24*, 1033–1045.

Pang, K.C., Frith, M.C., and Mattick, J.S. (2006). Rapid evolution of noncoding RNAs: lack of conservation does not mean lack of function. Trends Genet. *22*, 1–5.

Parker, B.J., Moltke, I., Roth, A., Washietl, S., Wen, J., Kellis, M., Breaker, R., and Pedersen, J.S. (2011). New families of human regulatory RNA structures identified by comparative analysis of vertebrate genomes. Genome Res. *21*, 1929–1943.

Pawlicki, J.M., and Steitz, J.A. (2008). Primary microRNA transcript retention at sites of transcription leads to enhanced microRNA production. J. Cell Biol. *182*, 61–76.

Pontier, D.B., and Gribnau, J. (2011). Xist regulation and function explored. Hum. Genet. *130*, 223–236.

Rossetto, C.C., and Pari, G. (2012). KSHV PAN RNA associates with demethylases UTX and JMJD3 to activate lytic replication through a physical interaction with the virus genome. PLoS Pathog. *8*, e1002680.

Sahin, B.B., Patel, D., and Conrad, N.K. (2010). Kaposi's sarcoma-associated herpesvirus ORF57 protein binds and protects a nuclear noncoding RNA from cellular RNA decay pathways. PLoS Pathog. *6*, e1000799.

Sasaki, J., Nakashima, N., Saito, H., and Noda, H. (1998). An insect picorna-like virus, Plautia stali intestine virus, has genes of capsid proteins in the 3′ part of the genome. Virology *244*, 50–58.

Schmid, M., and Jensen, T.H. (2010). Nuclear quality control of RNA polymerase II transcripts. Wiley Interdiscip Rev RNA *1*, 474–485.

Sharma, N., Ogram, S.A., Morasco, B.J., Spear, A., Chapman, N.M., and Flanegan, J.B. (2009). Functional role of the 5′ terminal cloverleaf in Coxsackievirus RNA replication. Virology *393*, 238–249.

Stadler, P.F. (2010). Evolution of the long non-coding RNAs MALAT1 and MENβ/ε. In Advances in Bioinformatics and Computational Biology, C.E. Ferreira, S. Miyano, and P.F. Stadler, eds. (Rio de Janeiro, Brazil: Springer).

Sun, R., Lin, S.F., Gradoville, L., and Miller, G. (1996). Polyadenylylated nuclear RNA encoded by Kaposi sarcoma-associated herpesvirus. Proc. Natl. Acad. Sci. USA *93*, 11883–11888.

Telford, E.A., Watson, M.S., Aird, H.C., Perry, J., and Davison, A.J. (1995). The DNA sequence of equine herpesvirus 2. J. Mol. Biol. *249*, 520–528.

Thompson, D.M., and Parker, R. (2007). Cytoplasmic decay of intergenic transcripts in Saccharomyces cerevisiae. Mol. Cell. Biol. *27*, 92–101.

Ulitsky, I., Shkumatava, A., Jan, C.H., Sive, H., and Bartel, D.P. (2011). Conserved function of lincRNAs in vertebrate embryonic development despite rapid sequence evolution. Cell *147*, 1537–1550.

Wang, H.W., Sharp, T.V., Koumi, A., Koentges, G., and Boshoff, C. (2002). Characterization of an anti-apoptotic glycoprotein encoded by Kaposi's sarcoma-associated herpesvirus which resembles a spliced variant of human survivin. EMBO J. *21*, 2602–2615.

Wang, Z., Day, N., Trifillis, P., and Kiledjian, M. (1999). An mRNA stability complex functions with poly(A)-binding protein to stabilize mRNA in vitro. Mol. Cell. Biol. *19*, 4552–4560.

Washietl, S. (2010). Sequence and structure analysis of noncoding RNAs. Methods Mol. Biol. *609*, 285–306.

Zhong, W., and Ganem, D. (1997). Characterization of ribonucleoprotein complexes containing an abundant polyadenylated nuclear RNA encoded by Kaposi's sarcoma-associated herpesvirus (human herpesvirus 8). J. Virol. *71*, 1207–1212.

Zoll, J., Heus, H.A., van Kuppeveld, F.J., and Melchers, W.J. (2009). The structure-function relationship of the enterovirus 3′-UTR. Virus Res. *139*, 209–216.

Zuker, M. (2003). Mfold web server for nucleic acid folding and hybridization prediction. Nucleic Acids Res. *31*, 3406–3415.